Physica A 391 (2012) 4191–4205

Contents lists available at SciVerse ScienceDirect

Physica A

journal homepage: www.elsevier.com/locate/physa

Stabilizing transient nanopatterns in heterogeneous catalysis: A comprehensive explanation of the phenomenon

Sergio E. Mangioni *,[1], Roberto R. Deza [2]

IFIMAR Instituto de Investigaciones Físicas de Mar del Plata (CONICET–UNMdP), Facultad de Ciencias Exactas y Naturales, Universidad Nacional de Mar del Plata, Deán Funes 3350, (B7602AYL) Mar del Plata, Argentina

ARTICLE INFO

Article history:
Received 5 August 2011
Received in revised form 8 March 2012
Available online 24 April 2012

Keywords:
Stabilization by noise
Pattern formation

ABSTRACT

A pattern-formation mechanism driven by attractive forces—previously studied in the context of lateral interactions between adsorbates—is reassessed through a simplified model. In its original version, such a mechanism needed an additional chemical reaction to stabilize the pattern. Recently, that goal has been achieved by means of a particular multiplicative noise. However, many details of the mechanism have remained obscure. In order to clarify them, we resorted to a simplified model that reproduces qualitatively the results of the studies carried out on the complete model. Our analysis reveals that such a mechanism may largely transcend the context in which it was found.

1. Introduction

Nonequilibrium pattern formation in heterogeneous catalysis – namely, catalytic chemical reactions in adsorbates on metal surfaces – has been an active subject of research for nearly forty years. With the resolution achieved by *photoelectron emission microscopy* (PEEM), the characteristic length scales of the structures seen were larger than the reactants' diffusion lengths, hence the patterns were well described by reaction–diffusion models [1,2]. The development of novel experimental techniques such as *field ion microscopy* and fast *scanning tunneling microscopy* (STM) – allowing atomic resolution in real time – showed that fast kinetic processes typically led to nanoscale patterns [3–5].

On the theoretical side it was shown that these nanoscale patterns, may result from the interplay of reactions and (either direct or bulk-mediated) *attractive potential interactions* between adsorbate molecules (note that our assertion refers only to a single adsorbate on a regular surface) [6]. Through heuristic arguments at the beginning and by outlining a microscopic master equation later on, Ertl, Mikhailov and collaborators shaped and substantiated a *nonlocal* mesoscopic kinetic equation which properly describes the behavior of surface-adsorbed particles experiencing attractive lateral interactions [7–12]. Moreover, this kinetic equation can be written as a reaction–diffusion equation with field-dependent coefficients. Some of these papers also showed that when a nonequilibrium chemical reaction is incorporated, these patterns become stable and grow [10–12].

The emphasis in those works was however on the final result (the stability diagrams for nanopattern formation on adsorbed surfaces) rather than in the complete understanding of the process. As a consequence, much of the mechanism has remained obscure, to the degree that – except in works directly related to adsorption in surfaces – it usually escapes the general bibliographic cites in the literature on pattern formation. Apparently it is not regarded as a general mechanism,

* Corresponding author.
E-mail addresses: smangio@mdp.edu.ar (S.E. Mangioni), deza@mdp.edu.ar (R.R. Deza).
1 Member of CONICET and FCEyN-UNMdP, Argentina.
2 Member of FCEyN-UNMdP, Argentina.

0378-4371/$ – see front matter
doi:10.1016/j.physa.2012.04.012

but as a particularity of the studies on adsorbed surfaces. A reason may be that in the phenomenon of surface adsorption to which it was applied, the driving force behind this mechanism is *subdominant* as compared to the dominant drift force. In fact, without the additional chemical reaction, the patterns are not stabilized. In our opinion, the pattern formation mechanism hidden in the referred nonlocal mesoscopic kinetic equation is far more general than what can be inferred at a first look.

During the last years – following the trend of change in the perception of the role of noise in Nature, from an unfailing destroyer to a possible (and frequent) builder of order [13–15] – also studies on noise-stabilized patterns have been carried out. These results belong to the realm of the so-called *noise-induced phase transitions*, which can be classified into two types: (a) the ones that originate in a short-time instability [16–21], and (b) those for which the disordered phase is stable at short times but destabilizes at long times, giving rise to phase transitions toward more orderly states [22–24]. Zero-dimensional systems can undergo transitions (although not *phase* transitions) of the second type, but not of the first one. Studies have been published on pattern formation based on both types of transitions [14]. For the sake of this work, it is the second type of phase transitions the relevant one. Some illustrative works in this respect have been published [25–28].

In a recent paper, a pattern formation mechanism driven by attractive forces and stabilized by means of a particular multiplicative noise was analyzed in detail [29]. The special role of the noise was to confine the system into a region of the field's configuration space where such a mechanism is enabled, causing this way the stabilization of the pattern. Such an effect was illustrated with the aforementioned model describing a system with attractive lateral interactions between adsorbates [7–9,30–32]. Initially, a situation in which the attractive forces do not achieve by themselves pattern stabilization was considered. This fact characterizes in general the effect of attractive lateral interactions between particles adsorbed on a surface. This way, incorporating an additional effect as e.g. a simple chemical reaction [10] or a multiplicative noise [29], the pattern can be stabilized (second type of the aforementioned phase transitions). This additional effect displaces the stationary homogeneous solution (hereafter, SHS) toward a region in configuration space which we shall call "constructive", or "domain of the attractive forces" (DAF), characterized by a *negative* (effective) *diffusion coefficient* and where the aforementioned mechanism is enabled. Such effective diffusion coefficient (D_{eff}) is the sum of those two effects of most relevance for the evolution of the pattern: that of true diffusion (which tends to homogenize it and produces a current proportional to the concentration gradient) and that of attractive lateral interactions which build it up (with a current whose form is not linear with concentration and tends to gather the adsorbates). It should be noted that the fact that $D_{eff} < 0$ does not mean a violation of the second law of thermodynamics, since it does not represent a real diffusion coefficient. As mentioned before, only expresses the sum of the real process of diffusion and the constructive effect driven by the attractive forces, contrary to the previous. However, the equation that models this phenomenon is so cumbersome that it limits the possibility to advance with the analytical work, so hindering the interpretation of the process. For that reason, we intended to simplify the problem. A brief report explaining the main idea has been has recently published [33]. We now make a extended paper explaining in detail the phenomenon. We have prioritized rescuing the essential characteristics of this phenomenon, to be able (at the cost of giving up in accuracy) to advance in the understanding of the process that characterizes it. We attempt to answer to questions such as

1. *Which effect is the most relevant one for the process of pattern buildup?*
2. *Why do we need, in order to stabilize the pattern, an additional effect that moves the SHS toward the constructive region or DAF?*
3. *How are the DAF and the dominant attractor's basin related?*
4. *Can the SHS and the pattern be simultaneously linearly stable?*
5. *How does the stability of the pattern depend on the parameters of the model?*

In Section 2 we outline a simplified model (introduced somewhere else [33] but reproduced here for completeness) that allows to put into evidence the most relevant aspects of this phenomenon, and show preliminary results that will be better sustained in the following section. In Section 3 we perform a stability analysis of the possible solutions that will enable answering the outlined questions, plus some others raised during the development. Finally, the conclusions are gathered in Section 4.

2. Simplified model

2.1. Some background

We assume a mesoscopic approach in one spatial dimension, and consider a field $\phi(x, \tau)$ – with ϕ and τ dimensionless variables – describing the *average* dynamics of some process. $\phi(x, \tau)$ is submitted to Refs. [29,32,33]

- a dimensionless drift force $Q_b(\phi)$ with at least one finite attractor (which determines the SHS in the absence of multiplicative noise),
- diffusion with normalized coefficient L^2_{dif},
- and some attractive interaction which creates a current *J toward x*, capable of generating a static *pattern* (periodic field configuration) outside the attractor's basin.

$Q_b(\phi)$ may have more than one attractor (depending on the parameters) but all of them must have their basins outside the DAF, where the attractive forces are successful in pattern buildup. The latter are assumed to stem from some short-range potential like, e.g., Ref. [10]

$$v(x) = (v_0/r_0)\exp[-(x/r_0)^2],$$

where $r_0 \ll L_{\mathrm{dif}}$ and $v_0 \equiv V_0/k_BT$ is dimensionless. *For a given pattern shape*, the term involving J can be cast as a field-dependent diffusion term by writing

$$J(x) \coloneqq L_{\mathrm{dif}}^2 G(\phi)\partial_x U_\phi,$$

where

$$U_\phi(x) \coloneqq \int \mathrm{d}x' v(x'-x)\phi(x')$$

is a (dimensionless) function of x but a *functional* of ϕ. $J(x)$ represents the current driven by attractive forces (it has nothing to do with real diffusion); moreover, by definition, $G(\phi) \geq 0$. This form allows to lump the diffusion processes and attractive interactions together into an *effective* diffusion coefficient [32]

$$D^*(\phi) \coloneqq 1 - \epsilon\, G(\phi),$$

which is dimensionless and both a function and a functional of ϕ. When $D^* > 0$ (hereafter, "domain of the diffusive process" or DDP), the effective diffusion term tends to homogenize the pattern; for $D^* < 0$ (DAF), it favors its buildup. The effective parameter

$$\epsilon \coloneqq \frac{\partial_x U_\phi}{\partial_x \phi}$$

(a positive functional of ϕ) represents the relative weight of the attractive forces with regard to temperature.

An example is lateral attractive interactions between particles adsorbed on a metallic surface where $0 \leq \phi(x,\tau) \leq 1$ is the local surface covering, $G(\phi) = \phi(1-\phi)$ since J is due to the attractive interaction (which requires x to be neither empty nor completely filled in a coarse-grained approximation), $r_0 \approx 1$ nm and $L_{\mathrm{dif}} \approx 1\,\mu$m [10,12].

As a matter of fact, if the attractive interactions are *subdominant* with respect to $Q_b(\phi)$ as in the present case, the ingredients introduced up to now do not in general suffice (even for $D^* < 0$) to render stable patterns, and the latter are only *transient*. The pattern will grow and develop from a finite harmonic perturbation of the SHS but finally, the attractor will drag it toward the DDP, where it will be washed out. In order to stabilize them, a third effect must be included. One possibility is a (first-order) *nonequilibrium* chemical reaction, whose product is immediately removed [10]. This was proposed in the context of lateral attractive interactions between adsorbates, and can actually represent either a photoinduced desorption or a bimolecular reaction where the second species reacts directly from the gas phase (Eley–Rideal mechanism).

A recently explored alternative (proposed within the same context) is a somewhat tailored multiplicative noise, namely a Gaussian white noise with zero mean $\eta(x,t)$ whose intensity is proportional to some control parameter λ, and which enters the field Langevin equation multiplying a function $\sqrt{\Gamma(\phi)}$ of the field [22,32,29,33]. This multiplicative noise induces an average drift $-\lambda\,\mathrm{d}\Gamma/\mathrm{d}\phi$. Hence the average behavior becomes described by equation:

$$\frac{\partial}{\partial\tau}\phi = Q(\phi) + L_{\mathrm{dif}}^2\frac{\partial}{\partial x}\left[D^*\frac{\partial\phi}{\partial x}\right], \tag{1}$$

being $Q(\phi) \coloneqq Q_b(\phi) - \lambda\,\mathrm{d}\Gamma/\mathrm{d}\phi$. The form of $\Gamma(\phi)$ is chosen in such a way that one of the attractors of $Q(\phi)$ (there can appear new ones) lies in the DAF ($D^* < 0$). This way, the corresponding SHS can be destabilized by a small inhomogeneous perturbation (in particular, a harmonic profile with wavenumber around some typical value k) [29]. We comment in passing that for $\lambda = 0$, Eq. (1) can be mapped into a relaxational dynamics one, where the relaxation coefficient is in fact $\Gamma(\phi)$ [32,29]. This form allows on one hand to incorporate the noise in such a way that the fluctuation–dissipation relation be satisfied [22,23], and on the other a simple resolution of the corresponding Fokker–Planck equation.

Although we firmly believe our results to be applicable to any case involving attractive interactions, for the sake of concreteness we illustrate this work with the case of attractive lateral interactions between adsorbed monomers, and choose [29]

$$\Gamma(\phi) \coloneqq (\phi - 0.5)^2 D_0^* + C, \tag{2a}$$

$$Q_b(\phi) \coloneqq \alpha(1-\phi) - \phi\exp(-U_\phi). \tag{2b}$$

- In Eq. (2a) it is $D_0^* = 1 - \epsilon_0 G(\phi)$, with ϵ_0 defined below, and C a constant guaranteeing $\Gamma(\phi) \geq 0$. The multiplicative factor $\Gamma(\phi)$ makes the noise very strong in the DDP and negligible in the DAF. This way, the system is pushed toward the region where the SHS can be destabilized by a small inhomogeneous perturbation, thus allowing the attractive interactions to build a stable pattern.

- The dimensionless parameter $\alpha > 0$ in Eq. (2b) has the original meaning $\alpha = k_a p_g / k_{d,0}$, where k_a is the sticking coefficient, $k_{d,0}$ the desorption rate in the absence of lateral interactions, and p_g the partial pressure of the gas phase (kept constant). The function $Q_b(\phi)$ resembles the typical cubic equation generally used in describing nonlinear systems.

Our idea is to retrieve a simplified form of Eq. (1) for the specific case of attractive lateral interactions in adsorbed surfaces, to show that this form qualitatively reproduces the behavior described by Eq. (1) and then to replace $Q_b(\phi)$ by a cubic normal form which will hopefully allow to reach farther in the analytic calculation. It will be seen that this cubic form does not change the quality of the results.

2.2. The main simplification

The shape of the numerically found solutions to Eq. (1) is most often approximately harmonic, with a profile oscillating around a constant value $\phi_0 \sim 0.5$ [10,29,32]. Assuming this shape, we parameterize the field as

$$\phi(\tau, x) = \phi_0(\tau) + \delta\phi_k(\tau) \sin kx. \tag{3}$$

In such a case, the functionals U_ϕ and ϵ (and with them Q_b and D^*, which are moreover functions of ϕ itself) become simply *functions* of the wavenumber k. In particular, ϵ becomes essentially the Fourier transform of the potential $v(x)$ of the attractive forces [29,32]

$$\epsilon(k) = \epsilon_0 \exp[-(kr_0/2)^2],$$

where ϵ_0 (its value for $k \ll r_0^{-1}$) is simply related to v_0. In order to get rid of the parameter L_{dif}, *we use it as the unit of length*. Adopting the quoted values of r_0 and L_{dif}, we choose to measure x in μm, and thus k in μm^{-1}.

The parameterization of $\phi(\tau, x)$ in Eq. (3) yields an explicit statement for $F(\tau, x)$ in Eq. (1) but otherwise, it does not simplify its treatment any further. An enormous simplification comes out however, by assuming that the relevant effects that intervene in the pattern's buildup and in the forces which tend to destabilize it *are summarized in their extrema and zero* (this is in fact the *main assumption* in this work). The restriction of Eq. (1) to these key points yields

$$\partial_\tau \phi_+ = Q_+(k) - k^2 D^*_+(k)\delta\phi_k, \tag{4a}$$

$$\partial_\tau \phi_- = Q_-(k) + k^2 D^*_-(k)\delta\phi_k, \tag{4b}$$

$$\partial_\tau \phi_0 = Q_0(k) + 2\epsilon(k)(\phi_0 - 0.5)k^2\delta\phi_k^2, \tag{4c}$$

with $\phi_\pm := \phi_0 \pm \delta\phi_k$, $Q_\bullet(k) := Q(k, \phi_\bullet)$, and

$$D^*_\pm(k) := D^*(k, \phi_\pm) = 1 - \epsilon\phi_0(1 - \phi_0) + \epsilon\delta\phi_k^2 \pm 2\epsilon(\phi_0 - 0.5)\delta\phi_k. \tag{5}$$

Although one of them is obviously redundant, each equation rescues an effect that is not present in the remaining ones. Depending on the sign of $D^*_\bullet(k)$, Eqs. (4a) and (4b) represent the tendency to make $\delta\phi_k$ grow ($D^* < 0$ region or DAF) or disappear ($D^* > 0$ region or DDP). Eq. (4c) tends to counteract this effect by moving ϕ_0 away from 0.5, dragging it toward the root of $Q(\phi) = 0$ and causing as a consequence the elimination of the pattern.

In order to obtain an evolution equation for the amplitude $\delta\phi_k(\tau)$ of the harmonic profile, we subtract (4b) from (4a). On the other hand, the evolution of ϕ_0 is better described by adding to (4c), half the sum of (4a) and (4b). This yields

$$\partial_\tau \phi_0 = Q_u - k^2 D^*_r \delta\phi_k + 2\epsilon(k)(\phi_0 - 0.5)k^2\delta\phi_k^2, \tag{6a}$$

$$\partial_\tau \delta\phi_k = Q_r - k^2 D^*_p \delta\phi_k, \tag{6b}$$

with $Q_u := Q_0 + \frac{1}{2}(Q_+ + Q_-)$, $D^*_p := \frac{1}{2}(D^*_+ + D^*_-)$, and $(\bullet)_r := \frac{1}{2}[(\bullet)_+ - (\bullet)_-]$ all functions of k. From Eq. (5), $D^*_p = 1 - \epsilon\phi_0(1 - \phi_0) + \epsilon\delta\phi_k^2$ and $D^*_r = 2\epsilon(\phi_0 - 0.5)\delta\phi_k$. Hence Eq. (6a) turns out to be simply $\partial_\tau\phi_0 = Q_u(k)$.

In order to verify the qualitative similarity between the processes (pattern formation and stabilization in the DAF, its elimination in the DDP) described respectively by Eqs. (6) and by Eq. (1), the evolution of ϕ_0 and $\delta\phi_k$ in Eqs. (6) was followed and contrasted with the results of simulations of Eq. (1), for different initial values of ϕ_0 but always starting from $\delta\phi_k = 10^{-5}$. The chosen values for the parameters were $\lambda = 1$, $\epsilon_0 = 5$, $r_0 = 10^{-3}$ μm and $k = 2\pi \times 10^2$ μm^{-1} (which yields a pattern wavelength of 10^{-2} μm, see Fig. 4). Figs. 1 and 2 show the evolution of ϕ_+ and ϕ_0 for a case in which the pattern is stabilized ($\alpha = 0.1$). The initial condition in Fig. 1 is $\phi_0 = 0.5$ (condition A) and in Fig. 2 it is $\phi_0 = 0.667$ (condition B, very near to the SHS). Fig. 3 also corresponds to the initial condition A of Fig. 1, but for a case in which the pattern is *not* stabilized ($\alpha = 0.15$) and the system evolves quickly toward the SHS (the same was observed starting from condition B).

The displayed curves reproduce qualitatively the behavior found in the numerical simulations of the Langevin equation whose deterministic part is shown in Eq. (1) [29]. For the case in Fig. 1 (stabilized pattern and condition A) ϕ_0 becomes constant somewhat above 0.5, while ϕ_+ increases abruptly at the beginning (because $\delta\phi_k$ jumps), reaches a plateau which presents an almost imperceptible maximum (not appreciable in Fig. 1) to finally become constant somewhat above the boundary separating the DAF from the DDP. This was also seen (although at much longer evolution times) in the numerical simulation of the stochastic process associated to Eq. (1). For the case in Fig. 3 (condition A but pattern *not* stabilized) ϕ_+

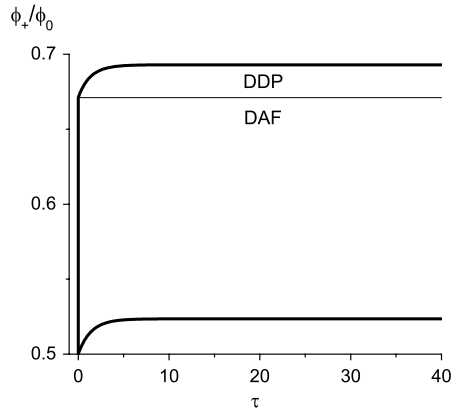

Fig. 1. ϕ_+ (upper curve) and ϕ_0 (lower curve) *vs.* τ. Case in which the pattern is stabilized ($\alpha = 0.1$) and initial condition A ($\phi_0 = 0.5$, $\delta\phi_k = 10^{-5}$). Remaining parameters: $\lambda = 1$, $\epsilon_0 = 5$, $r_0 = 10^{-3}$ μm, and $k = 2\pi \times 10^2$ μm^{-1}. The horizontal line indicates the boundary between the DAF (below it) and the DDP (above it).

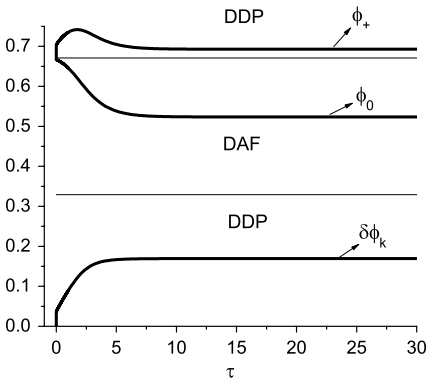

Fig. 2. ϕ_+ (upper curve), ϕ_0 (central curve) and $\delta\phi_k$ (lower curve) *vs.* τ. Case in which the pattern is stabilized (parameters as in Fig. 1) and initial condition B ($\phi_0 = 0.667$, $\delta\phi_k = 10^{-5}$). The DAF lies between the horizontal lines, and the DDP outside them.

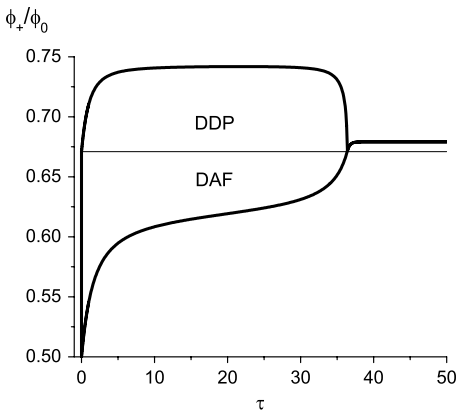

Fig. 3. ϕ_+ (upper curve) and ϕ_0 (lower curve) *vs.* τ. Case in which the pattern is *not* stabilized ($\alpha = 0.15$) and initial condition A ($\phi_0 = 0.5$, $\delta\phi_k = 10^{-5}$). Remaining parameters as in Fig. 1. The horizontal line indicates the boundary between the DAF (below it) and the DDP (above it).

also reaches a plateau after an abrupt growth; nevertheless, since simultaneously ϕ_0 is driven toward the attractor, ϕ_+ falls abruptly to merge with ϕ_0 ($\delta\phi_k$ vanishes abruptly) and they proceed slowly together toward the attractor until finally reaching it. This evolution was also observed (although at much longer evolution times) in the numerical simulation of the stochastic process associated to Eq. (1). For the case in Fig. 2 (stabilized pattern and condition B), the curves show that while $\delta\phi_k$ grows, *the pattern is pushed toward the center of the DAF*, until the stationary pattern is reached with ϕ_0 somewhat above 0.5. The existence of a maximum in $\phi_+(\tau)$ evidences the *strong* initial constructive drive of the attractive interactions. This

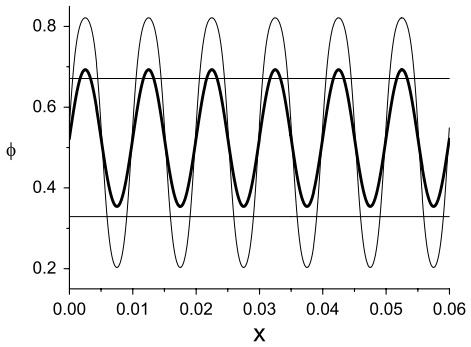

Fig. 4. Pattern calculated with the extended system (thin line) and with the simplified model (thick line), for the parameters in Fig. 1. The DAF lies between the horizontal lines, and the DDP outside them.

behavior was also observed in the extended system [29], where it was described as a rebound against the "noise wall" of the growing pattern.

Fig. 4 shows the difference in amplitude existing between the pattern predicted by this simplified model (thick line) and the one calculated with the extended system. By considering together the equations that describe the simplified model and the previous figures, one understands that the pattern is built by the drive of the attractive interactions *at the ends* ϕ_+ and ϕ_-, which according to Eq. (6b) – or equivalently, Eqs. (4a) and (4b) – make $\delta\phi_k$ grow (by pulling the pattern from the ends) for $D_p^* < 0$. For the extended system described by Eq. (1), such a constructive drive acts *on the whole profile* (except at ϕ_0) and therefore a larger-amplitude pattern is expectable. The upward displacement of the pattern (ϕ_0 lies somewhat above 0.5) is due to the inherent *asymmetry* of $Q_b(\phi)$ in Eq. (2b).

For initial condition A, in both cases analyzed, the construction of a pattern is observed. While in the first case (Fig. 1) it subsists, in the second (Fig. 3) it does not. The essential difference between these two cases is that in the first one, the SHS is located in the DAF, whereas in the second, it is in the DDP. The attractive forces act constructively under both circumstances, but they do not by themselves succeed to stabilize the built pattern. Some effect is required that moves the SHS toward the DAF (in our case, a multiplicative noise which is strong enough in the DDP and almost imperceptible in the DAF).

The usual approach to stability is: "a pattern with a given k will stabilize *if the SHS is unstable* under a perturbation with that k" [10,29]. This is true, but it can also be true that both (the SHS and the pattern) be linearly stable for the same set of parameters. If the SHS can be destabilized by a perturbation with a wavenumber k' different to that of the pattern, another pattern with that k' is expected to finally become stable. Nevertheless, if it is possible to force a value of k through the boundary conditions, such a bistable circumstance (between pattern and SHS) could be possible.

6. *If the SHS is linearly stable under any perturbation* (*whatever its k*), *can one expect that no pattern be stabilized?*

2.3. A further simplification

In short, we try to understand more clearly the process that leads to the construction of these patterns and, according to the case, the one that stabilizes or destabilizes them. To that end we notice that the nonlinearity $Q_b(\phi)$ in Eq. (2b) is similar in shape to a cubic equation [29]. So, with the aim of advancing as far as possible with the analytic calculation, and assuming that it is the *number and types of roots* of $Q_b(\phi) = 0$ (and not its detailed shape) what determines the system's behavior in a given parametrical regime, we define $u := \phi - 0.5$ and propose $Q_b(u) := u(\alpha - u^2)$. This simpler expression – with which numerous nonlinear phenomena have been described – shares with Eq. (2b) the possibility of exhibiting two attractors and a saddle (depending on α). But at variance with Eq. (2b), which had no definite symmetry and contained U_ϕ, it is independent of k and has its attractors $\pm\sqrt{\alpha}$ symmetrically located. Since from Eq. (2a) it is

$$\lambda \frac{\mathrm{d}\Gamma(\phi)}{\mathrm{d}\phi} = 2\lambda u \left(1 - \frac{\epsilon_0}{4} + 2\epsilon_0 u^2\right),$$

the simpler nonlinearity with the incorporated noise-induced drift can be written as $Q(u) = u(\omega - r_{nl}u^2)$ with $\omega := \alpha + 2\lambda p_0$, $r_{nl} := 1 + 4\lambda\epsilon_0$ and $p_0 := \epsilon_0/4 - 1$. Hence

$$Q_u = u_0[2\omega - r_{nl}(2u_0^2 + 3\delta\phi_k^2)],$$
$$Q_r = u_0[\omega - r_{nl}(3u_0^2 + \delta\phi_k^2)].$$

In terms of $u_0 := \phi_0 - 0.5$, $D_p^* = 1 - \epsilon(0.25 - u_0^2) + \epsilon\delta\phi_k^2$ and Eqs. (6) read

$$\partial_\tau u_0 = u_0[2\omega - r_{nl}(2u_0^2 + 3\delta\phi_k^2)], \tag{7a}$$

$$\partial_\tau \delta\phi_k = \delta\phi_k \begin{Bmatrix} \omega - r_{nl}(3u_0^2 + \delta\phi_k^2) \\ -k^2[\epsilon(k)(u_0^2 + \delta\phi_k^2) - p(k)] \end{Bmatrix}. \tag{7b}$$

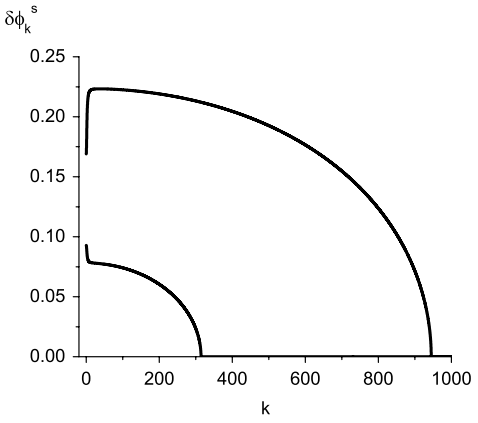

Fig. 5. Amplitude of the pattern *vs.* k (in $\mu\mathrm{m}^{-1}$) for $\epsilon_0 = 5$ (upper curve) and $\epsilon_0 = 4.1$ (lower curve). Remaining parameters as in Fig. 1.

$p(k) := \epsilon(k)/4 - 1$ is a relevant parameter whose sign change defines a critical limit. For $p(k) > 0$, which process prevails will depend on the sign of D^* for that k, as already established. For $p(k) < 0$ instead, the constructive process is *inhibited for all possible initial values* of ϕ_0 and $\delta\phi_k$ (for a given k), prevailing homogenization by diffusion. Since ϵ (and thus p) are decreasing functions of k, it suffices that $p_0 < 0$ (namely $\epsilon_0 < 4$) to inhibit the constructive process for all k. This means that *even in the presence of noise*, the attractive lateral interactions will never have enough strength to overcome the diffusion process. This is so because the larger λ, the smaller ω will be (it can even become $\omega < 0$ for $\lambda > \alpha/2|p_0|$). Note moreover that the absence of terms proportional to k^2 in Eq. (7a) – because both terms in Eq. (6a) cancel each other – is a relevant effect for the stabilization of the pattern, that is effective only in the DAF. This way it becomes evident from Eq. (7a), that the force tending to destabilize the pattern is just the drift of ϕ_0 toward the attractor.

The stationary solutions, $u^s(x) = u_0^s + \delta\phi_k^s \sin kx$, of Eqs. (7) are

(a) The trivial one ($u_0^s = 0$, $\delta\phi_k^s = 0$);
(b) Two nontrivial SHS

$$u_0^s = \pm\sqrt{\omega/r_{nl}}, \qquad \delta\phi_k^s = 0, \tag{8}$$

as far as $0 < \omega < r_{nl}/4$;
(c) Two centered, phase-conjugate patterns

$$u_0^s = 0, \qquad \delta\phi_k^s = \sqrt{\frac{\omega + k^2 p(k)}{r_{nl} + k^2\epsilon(k)}}, \tag{9}$$

as far as $0 < \omega + k^2 p < (r_{nl} + k^2\epsilon)/4$;
(d) Four eventual solutions with both u_0^s and $\delta\phi_k^s$ different from zero.

In this work, we focus on solutions (b) and (c). For $\lambda = 0$, they become $u_0^s = \pm\sqrt{\alpha}$, $\delta\phi_k^s = 0$ as far as $\alpha < 1/4$, and $u_0^s = 0$, $\delta\phi_k^s = \sqrt{\frac{\alpha + k^2 p}{1 + k^2\epsilon}}$ as far as $0 < \alpha + k^2 p < (1 + k^2\epsilon)/4$. Numerical evaluation (by following the evolution of ϕ_0 and $\delta\phi_k$ for parameter values in that range) reveals that the latter are stable only below $k \sim 2\pi \times 10^1\ \mu\mathrm{m}^{-1}$ (a smoother pattern) and $\epsilon_0 \sim 10$ (larger than the value used in the figures). For these parameter values, the SHS for this simplified system ($u^s = \pm\sqrt{\omega/r_{nl}}$) falls in the DAF for a band around $k \sim 2\pi \times 10^1\ \mu\mathrm{m}^{-1}$. Contrarily, for larger k ($\sim 2\pi \times 10^2\ \mu\mathrm{m}^{-1}$) and/or smaller ϵ_0 (~ 5), the SHS is located in the DDP, and the pattern is unstable. This can be verified. This will become clearer in the next section, through the stability analysis. A point worth noticing is that Eq. (8) coincides with the SHS of the extended system for this nonlinearity.

Let us assume $p_0 > 0$ (namely $\epsilon_0 > 4$) and consider Eq. (9). Both ϵ and p are decreasing functions of k, but $p(k)$ *will change sign* at a value of k which depends on ϵ_0 and r_0. Then for slightly larger values of k such that $|p(k)| > \omega/k^2$, $\delta\phi_k^s$ becomes imaginary (i.e. the pattern ceases to be a solution of the system). Numerically, this is seen to occur for $p \sim 0$ i.e. just at the threshold beyond which the constructive process is inhibited for all possible initial values of ϕ_0 and $\delta\phi_k$. Fig. 5 shows two representative plots of the stationary amplitude $\delta\phi_k^s$ of the pattern *vs.* k. The pattern is a possible solution only within a band between $k = 0$ and the wavenumber for which $\delta\phi_k^s = 0$. Beyond that value, ϕ_0^s ends up coinciding with the SHS.

For small k, a first-order expansion of Eq. (9) in powers of k^2 yields

$$\delta\phi_k^s \approx \sqrt{\frac{\omega}{r_{nl}}}\left[1 + \frac{k^2}{2}\left(\frac{p_0}{\omega} - \frac{\epsilon_0}{r_{nl}}\right)\right],$$

indicating an initial quadratic departure from $\delta\phi_{k=0}^s$ (which coincides with the SHS) with a growth rate given by $p_0/\omega - \epsilon_0/r_{nl}$, until the condition $pr_{nl} = \omega\epsilon$ (for the vanishing of the first derivative of $\delta\phi_k^s$ with respect to k) is met. For $\lambda = 1$ and $\alpha = 0.1$

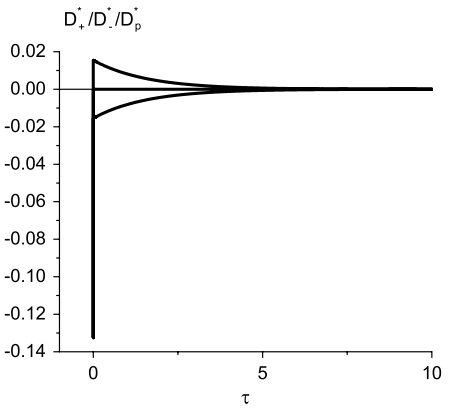

Fig. 6. D^*_+ (upper curve), D^*_- (lower curve) and D^*_p (central curve) *vs.* τ for the cubic nonlinearity. Case in which the pattern is stabilized ($\alpha = 0.1$) and initial condition ($\phi_0 = 0.51, \delta\phi_k = 10^{-5}$). Remaining parameters as in Fig. 1. In this timescale, the three curves appear superimposed at the beginning and at the end of the process. The difference is appreciable only in the central stage. $D^*_r(\tau)$ (not shown) coincides with $D^*_+(\tau)$ in this timescale.

the condition $p_0 r_{nl} = \omega\epsilon_0$ is met at $\epsilon_0^* = 4.17863$. Accordingly, the curves present a qualitative difference depending on $\epsilon_0 - \epsilon_0^*$:

- For $\epsilon_0 < \epsilon_0^*$, the curves show an initial abrupt fall at $k \sim 0$, drawing afterwards an approximately quarter-circular arch (a clear signal that the k^2-terms rule), until becoming zero at a not too large value of k.
- For $\epsilon_0 > \epsilon_0^*$, there is an initial abrupt rise of the curve until a maximum is quickly being reached; then, as in the previous case, the amplitude of the pattern decreases to zero ($p = 0$) drawing an approximately quarter-circular arch, but of quite larger radius than in the previous case.

Variations of the parameters λ or α do not lead to qualitative changes in the curves. They only change the value of ϵ_0^*. Notice that the zero amplitude is reached for k values whose inverse is of the order of the interaction range. It is also pertinent to highlight that a similar behavior (although circumscribed to small k's) is observed even when $\lambda = 0$.

7. *What causes the amplitude of the pattern to saturate at a given value when it is stable, or to decrease to zero after reaching a maximum when it is unstable?*

Our preliminary analysis tells us that this is linked to the location of the SHS. If it is in the DAF the pattern is stabilized, while the SHS is not; and if it is in the DDP, the pattern is not stabilized but the SHS is.

8. *But how and why does this circumstance occur?*
9. *Is it always one or the other? Cannot both have their niche in different attraction basins, and compete for relative stability?*

Since we have established that the constructive drive is effective whenever $D^* < 0$, we found it appropriate to observe the evolution of D^*_+, D^*_-, D^*_p and D^*_r for $k = 2\pi \times 10^2\ \mu\text{m}^{-1}$, starting from the initial condition ($\phi_0 = 0.51$, $\delta\phi_k = 10^{-5}$) until reaching the stationary state. From Eqs. (8) and (9) it is

$$D^{*s}_p = D^{*s}_\pm = -p(k) + \epsilon(k)\omega/r_{nl}, \qquad D^{*s}_r = 0,$$
$$D^{*s}_p = D^{*s}_\pm = -p(k) + \epsilon(k)\delta\phi^{s\,2}_k, \qquad D^{*s}_r = 0$$

for the SHS and the pattern respectively. The values of D^{*s}_p for the parameters in Figs. 6–8 are respectively 0.066563 and -3.62999×10^{-8}.

Fig. 6 shows the evolution of D^*_+, D^*_-, and D^*_p when the pattern is stable (the SHS falls in the DAF). D^*_+ and D^*_- are initially strongly negative, and they overlap due to the smallness of $\delta\phi_k$. The violent rise of $\delta\phi_k$ – much faster than the vanishing of u_0 – makes D^*_+ and D^*_- depart from each other for a while. After the slow relaxation of u_0 toward zero, the balance between the attractive forces and the diffusion processes is established: all the effective diffusion coefficients become zero, and the pattern is stabilized. Since $D^*_p \approx 0$ after the strong initial rise, $D^*_r(\tau)$ overlaps with $D^*_+(\tau)$. Had the initial condition been $u_0 = u_0^s = 0$ (and $\delta\phi_k = 10^{-5}$), it had been $D^*_r(\tau) = 0$ even when $\delta\phi_k$ rose violently, and the other three curves would have overlapped during the whole evolution.

Fig. 7 plots D^*_+ and D^*_- *vs.* τ for the previous initial condition, but for a case in which the pattern is *not* stabilized (the SHS falls in the DDP). As in Fig. 6, D^*_+ and D^*_- differ only in a central stage after an initial abrupt increase during which they overlap. But at variance with Fig. 6 – characterized by the slow relaxation of u_0 toward zero – D^*_+ and D^*_- first depart even further from each other (following the slow relaxation of u_0 toward $\sqrt{\omega/r_{nl}}$) and then they quickly merge as $\delta\phi_k \to 0$, to continue following overlapped the slow relaxation of u_0.

Fig. 8 plots D^*_p and D^*_r *vs.* τ for the same case, showing that D^*_p exhibits a transient plateau at $D^*_p \approx 0$ while D^*_+ and D^*_- differ from each other. Again, $D^*_r(\tau)$ overlaps with $D^*_+(\tau)$. The fact that the stationary values of D^*_+, D^*_-, and D^*_p are positive shows that in this case, the attractive forces are not able to counter the diffusion process. A point worth noticing is that the

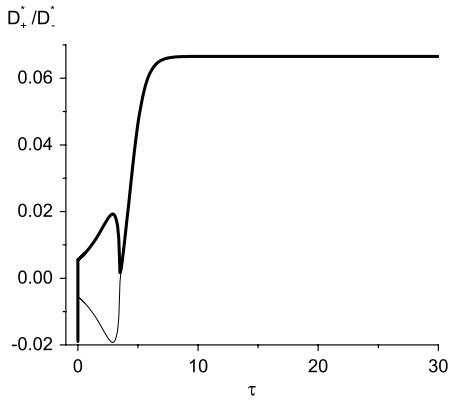

Fig. 7. D^*_+ (thick line) and D^*_- (thin line) *vs.* τ for the cubic nonlinearity. Case in which the pattern is *not* stabilized ($\alpha = 0.15, \epsilon_0 = 4.5$) and initial condition ($\phi_0 = 0.51, \delta\phi_k = 10^{-5}$). Remaining parameters as in Fig. 1. The curves differ only in the central stage, after an initial abrupt increase during which they appear superimposed. After this stage they continue to be superimposed until reaching the stationary state.

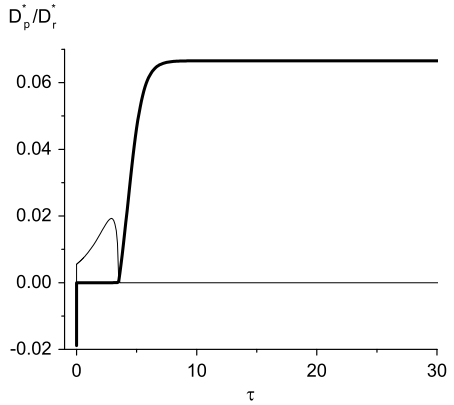

Fig. 8. D^*_p (thick line) and D^*_r (thin line) *vs.* τ for the cubic nonlinearity. Case in which the pattern is *not* stabilized ($\alpha = 0.15, \epsilon_0 = 4.5$) and initial condition ($\phi_0 = 0.51, \delta\phi_k = 10^{-5}$). Remaining parameters as in Fig. 1. The curves differ only in the central stage, after an initial abrupt increase during which they appear superimposed. After this stage they continue superimposed until reaching the stationary state.

maximum value of $D^*_+(\tau)$ – and hence of $D^*_r(\tau)$ – is ≈ 0.02 in both cases. Considering moreover that in the case of Fig. 6, the central stage (where the differences between the curves are noticeable) does not take place when starting from $\phi_0 = 0.5$, we can intuit that the bid between pattern and SHS is defined in this stage.

Finally, the fact that $D^*_\pm(u^s) = D^{*s}_p(u^s) > 0$ is obtained for $p(k) > 0$ tells us that bistable behavior between the pattern and the SHS is indeed possible for a given k. Figs. 9 and 10 show both evolutions for the same set of parameter values and different initial conditions. When the initial condition is ($\phi_0 = 0.66, \delta\phi_k = 10^{-5}$), the pattern is stabilized; contrarily, starting from a slightly higher value of ϕ_0 (and the same $\delta\phi_k$), the SHS is stabilized. The option between pattern and SHS is little sensible to variations of $\delta\phi_k$. The following stability analysis facilitates a better understanding of these results.

3. Bistability region

Two linear-stability analyses must be carried out: that of the pattern and that of the SHS. From the previous section, several possibilities can be expected. The pattern may be linearly stable but not the SHS, or vice versa. But also, both may be linearly stable, having each one its own basin of attraction.

3.1. Linear stability of the pattern

From Eqs. (7), the stationary pattern of Eq. (9) will be linearly stable under a homogeneous perturbation $\delta u\, e^{\Lambda\tau}$ (with $\delta u^2 \ll \delta\phi_k^{s2}$) if

$$\Lambda_1 = 2\omega - 3r_{nl}\,\delta\phi_k^{s2} < 0, \tag{10a}$$

$$\Lambda_2 = \omega - 3r_{nl}\,\delta\phi_k^{s2} - [3\epsilon\,\delta\phi_k^{s2} - p]k^2 < 0. \tag{10b}$$

These inequalities are of course fulfilled in Figs. 6–10.

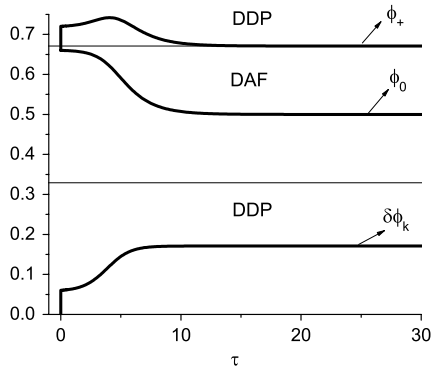

Fig. 9. ϕ_+ (upper curve), ϕ_0 (central curve) and $\delta\phi_k$ (lower curve) *vs.* τ for the cubic nonlinearity, and $\alpha = 0.15$. Remaining parameters as in Fig. 1. Case in which the pattern is stabilized: initial condition ($\phi_0 = 0.66$, $\delta\phi_k = 10^{-5}$). The DAF lies between the horizontal lines, and the DDP outside them.

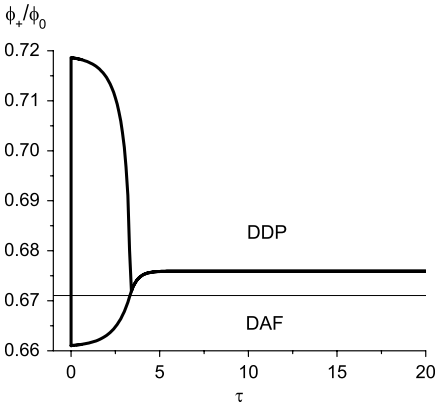

Fig. 10. ϕ_+ (upper curve) and ϕ_0 (lower curve) *vs.* τ for the cubic nonlinearity, and $\alpha = 0.15$. Remaining parameters as in Fig. 1. Case in which the pattern is *not* stabilized: initial condition ($\phi_0 = 0.661$, $\delta\phi_k = 10^{-5}$). The DAF lies below and the DDP above the horizontal line. The curves overlap when $\delta\phi_k$ (not shown) becomes zero.

As an illustration we consider the extreme cases, namely $k \to \infty$ ($\delta\phi_k^{s2} \to p/\epsilon$ and therefore $D_p^{*s} = D_r^{*s} = D_+^{*s} = D_-^{*s} = 0$) and $k \to 0$ ($\delta\phi_k^{s2} \to \omega/r_{nl}$, and the nonlinearity intervenes significantly in the balance of forces).

For large k, Λ_1 and Λ_2 can be written as

$$\Lambda_1 = 2\omega - \frac{3r_{nl}p}{\epsilon} < 0, \tag{11a}$$

$$\Lambda_2 = -2pk^2 < 0. \tag{11b}$$

In this circumstance, the requirement $p > 0$ for the pattern to be stabilized becomes evident. The pattern becomes *unstable* when $p < 0$ (which implies $\delta\phi_k^{s2} < 0$), i.e. when the constructive process is inhibited for all possible values of the field. From $\epsilon = \epsilon_0 \exp[-r_0^2k^2/4]$, it turns out that for k too large or ϵ_0 small enough, the pattern is destabilized. Recalling that $r_{nl} = 1 + 4\lambda\epsilon_0$, we see that the *average* effect of the noise is *to power up the constructive effect of the attractive forces* against the destabilizing effect of the nonlinearity (even when its influence in $\omega = \alpha + 2\lambda p_0$ appears to be the opposite, namely accompanying the nonlinearity). Notice moreover that if $\lambda = 0$, then $\omega = \alpha$ and $r_{nl} = 1$; hence it is clear that in the absence of multiplicative noise, a pattern can be stabilized whenever α is sufficiently small and ϵ_0 sufficiently large.

For small k, a Taylor expansion yields

$$\Lambda_1 = -\omega - 3[p - \omega\epsilon]k^2 < 0, \tag{12a}$$

$$\Lambda_2 = -2\omega - [2p - 3\omega\epsilon]k^2 < 0. \tag{12b}$$

Again, the attractive forces impel the constructive processes (in this case, with the help of the nonlinearity) and the noise has again a stabilizing effect.

Figs. 11 and 12 plot Λ_1 and Λ_2 *vs.* k for different values of ϵ_0. The transition from $p > 0$ to $p < 0$ – where $\Re(\Lambda)$ is taken – occurs after Λ_1 becomes positive, and little before Λ_2 does so. Hence, it is enough to look at Λ_1 to determine the band of values of k for which the pattern is stable, between 0 and a value whose inverse is of the order of the interaction range.

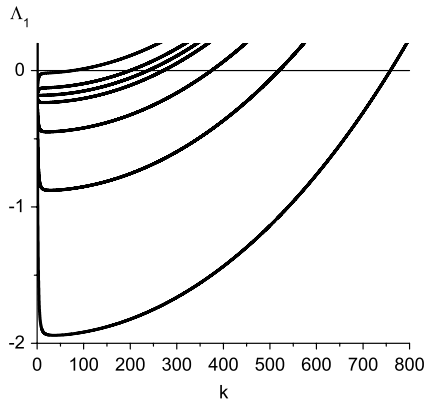

Fig. 11. Λ_1 *vs. k*, for ϵ_0 increasing from bottom to top (4.1, 4.15, 4.175, 4.2, 4.3, 4.5, 5.). $\lambda = 1$, $\alpha = 0.1$ and $r_0 = 10^{-3}$ μm. Λ_1 remains real in the whole plotted range, since the value of k causing p to change its sign is even larger.

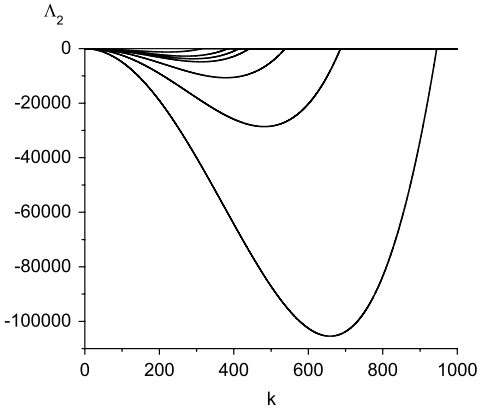

Fig. 12. Λ_2 *vs. k*, for ϵ_0 increasing from bottom to top (4.1, 4.15, 4.175, 4.2, 4.3, 4.5, 5.). $\lambda = 1$, $\alpha = 0.1$ and $r_0 = 10^{-3}$ μm. For $p < 0$ (which happens little before $\Lambda_2 > 0$) $\Re(\Lambda_2)$ is taken.

As ϵ_0 approaches its critical value ($\epsilon_0 = 4$), this band of k values narrows and approaches zero, until finally – when $\epsilon_0 \leq 4$ – any possibility to stabilize the pattern disappears. A similar behavior was observed for other values of α and λ. For a given α and different values of the noise intensity, the stability band does not change much for $\lambda > 0.5$, while it decreases quickly for smaller values. Nevertheless, a band of k values for which both Λ_1 and Λ_2 are simultaneously negative was observed even for $\lambda = 0$, although circumscribed to $k \sim 0$. This stability band widens as ϵ_0 increases. Regarding the Λ_2 *vs. k* curves, practically no differences are observed by varying either α or λ. This can be understood from Eq. (11b). Finally, the same qualitative change shown for the of $\delta\phi_k^s(k)$ curves (see Fig. 5) – as well as the fact that it happens around $k = 0$ (although with a sign inversion) – can also be observed in $\Lambda_1(k)$.

In general, it can be stated that for the pattern to be stabilized, the constructive process ($p > 0$) should be enabled for some value of $\delta\phi_k$. This is not the same as requiring the SHS to be located in the DAF: it is perfectly possible to have simultaneously $D^*(u^s) > 0$ and $p > 0$, as already shown for the case of Figs. 9 and 10.

3.2. Linear instability of the SHS

The stability analysis of the SHS is carried out by perturbing it with an infinitesimal harmonic profile – namely introducing $u^s + \delta u \exp[\Omega_k \tau] \exp[ikx]$ in Eq. (1) – and observing the effect of this perturbation on the SHS [29]. This way a curve $\Omega_k(k)$ is obtained, featuring a maximum for some k. This maximum can be negative or positive according to the value of the parameters characterizing the model. As it is known, an inhomogeneity with components whose k lie inside the band where $\Omega_k(k) > 0$, can destabilize the SHS. For this case $\Omega_k(k)$ adopts the form

$$\Omega_k = -2\omega - k^2 D^*(u^s). \tag{13}$$

Since the SHS of Eq. (8) is also solution of Eqs. (7), Eq. (13) can be obtained by carrying out a linear stability analysis of the SHS from these equations. For the proposed profile to destabilize the SHS, k should be such that $D^*(u^s) = \epsilon {u^s}^2 - p < 0$,

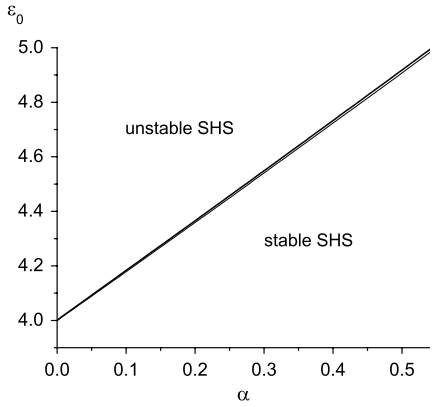

Fig. 13. ϵ_0 *vs.* α curves of exact (thin line) and approximate (thick line) stability of the SHS. $\lambda = 1$ and $r_0 = 10^{-3}$ μm. The instability region lies above the curves. Since $r_0 \ll \frac{1}{k_M}$, an almost full overlapping is observed of both curves.

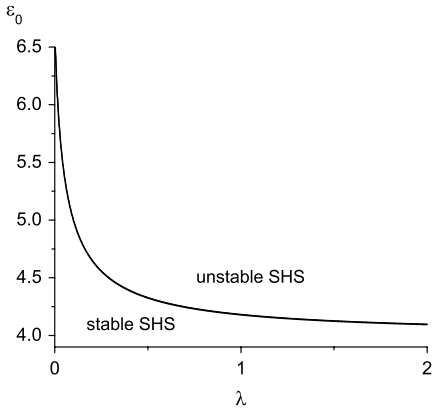

Fig. 14. ϵ_0 *vs.* λ curves of exact (thin line) and approximate (thick line) stability of the SHS. $\alpha = 0.1$ and $r_0 = 10^{-3}$ μm. The instability region lies above the curves. Since $r_0 \ll \frac{1}{k_M}$, an almost full overlapping is observed of both curves.

which means again $p > 0$. The boundary separating the region of parameter values where that can occur from the one where it cannot (stability curve) is calculated by considering the first mode (k_M) that destabilizes the SHS, solving

$$\Omega_k(k, \alpha, \epsilon_0, \lambda, r_0) = 0,$$
$$\partial_k \Omega_k(k, \alpha, \epsilon_0, \lambda, r_0) = 0.$$

This way we calculate the wavenumber corresponding to the first mode that destabilizes, obtaining

$$k_M^2 = -\omega + \sqrt{\omega^2 + 16\omega/r_0^2}. \tag{14}$$

When r_0 is small (as in our case) this expression can be approximated as

$$k_M^2 \approx 4\sqrt{\omega}/r_0. \tag{15}$$

Continuing in this direction, we find an approximate expression for the stability curve

$$\epsilon_0 \approx 2 + \frac{\alpha}{\lambda} - \frac{1}{4\lambda} + \sqrt{\left(2 + \frac{\alpha}{2\lambda} - \frac{1}{4\lambda}\right)^2 + \frac{2}{\lambda}}. \tag{16}$$

Figs. 13 and 14 show the stability curves (ϵ_0 *vs.* α and ϵ_0 *vs.* λ) calculated in exact and approximate form. An almost full overlap is observed between both calculation methods. Since an increase of α powers up the attractor, the attractive forces need to be more intense for the SHS to be destabilized. Recall that the noise was introduced in such a way that it weakens the attractor, moving it toward the constructive area. Then, as the noise intensity increases, a smaller intensity of the attractive forces is necessary to destabilize the SHS. Both behaviors are reflected in the curves of Figs. 13 and 14 and of course also in the expression (16).

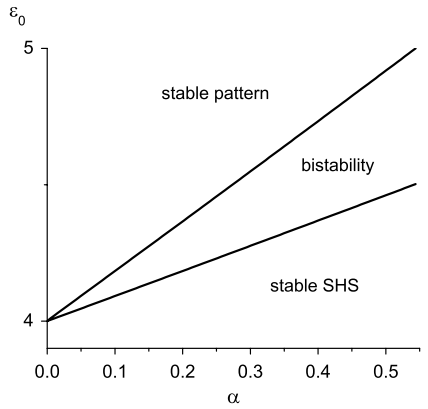

Fig. 15. Bistability region: ϵ_0 *vs.* α stability curves of the pattern (lower line), $k = 2\pi \times 10^1\ \mu\mathrm{m}^{-1}$ and of the SHS (upper line). $\lambda = 0.1$ and $r_0 = 10^{-3}\ \mu\mathrm{m}$. The bistability region it is located between the two curves.

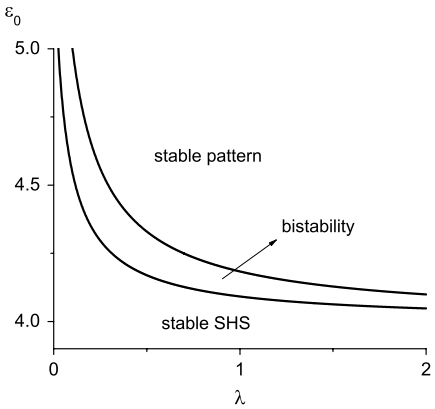

Fig. 16. Bistability region: ϵ_0 *vs.* λ stability curves of the pattern (lower line), $k = 2\pi \times 10^1\ \mu\mathrm{m}^{-1}$ and of the SHS (upper line). $\alpha = 0.1$ and $r_0 = 10^{-3}\ \mu\mathrm{m}$. The bistability region it is located between the two curves.

3.3. Nonlinear stability analysis

Now we are interested in ascertaining the possibility of a pattern-SHS *bistability*, the SHS being linearly *stable* under small inhomogeneities (parameter values *below* the curves of Figs. 13 and 14). To that end we calculate curves with $\Lambda_1(k, \alpha, \epsilon_0, \lambda, r_0) = 0$ and observe whether they lie below the curves of Figs. 13 and 14. In order to identify the bistability region, we must first obtain the stability curves of the pattern. From Eq. (11a) we obtain an analytic expression (valid for k large enough)

$$\epsilon_0 = \frac{\alpha}{2\lambda} - \frac{3}{16\lambda} - 1 + \frac{3}{\epsilon^*} + \sqrt{\left(\frac{\alpha}{2\lambda} - \frac{3}{16\lambda} - 1 + \frac{3}{\epsilon^*}\right)^2 + \frac{3}{2\lambda}}, \tag{17}$$

where $\epsilon^* = \epsilon/\epsilon_0$. The stability curves of the pattern are shown in Figs. 15 and 16, together with those of the SHS. For the first ones, $k = 2\pi \times 10^1\ \mu\mathrm{m}^{-1}$ was chosen (it was numerically verified that this value is large enough for the approximation to be valid). A region of parameter values is indeed observed to exist, where the referred bistability is possible. Such prediction was checked following several evolutions of Eqs. (7a) and (7b), selecting at random different sets of parameter values for which the system was in this region. In all the cases, both attraction basins – that of the SHS and that of the pattern – were found. Moreover, a similar (although quite simpler) calculation, allows to show that such a bistability is also possible in absence of noise.

Given the results with this nonlinearity, we explore the possibility of such a bistability for the original nonlinearity (adsorption and desorption in surfaces with attractive interactions). We take points very near to the stability curve of the SHS: [29] the same value of α, a value of ϵ slightly below the one corresponding to the curve and the first destabilizing mode for that point of the curve. For all cases, the system exhibited the same bistability that for the cubic nonlinearity.

3.4. A consequence

Now we will see that this mechanism pattern formation – based on the balance between attractive forces and homogenization by diffusion – is not only independent of the nonlinearity, but also that the latter is not necessary, nor is even any force at all! Let us begin considering, instead of the nonlinearity, a linear force $Q_b(u) = -\alpha u$. This way, the forms of the inequalities that indicate the pattern's and the SHS's stability conditions are the same as before, but replacing ω by $\omega_l = -\alpha + 2\lambda p_0$ and r_{nl} by $r_l = 4\lambda\epsilon_0$. Now, the inequalities indicating the pattern's stability read

$$\Lambda_1 = 2\omega_l - 3r_l\delta\phi_k^{s2} < 0, \tag{18a}$$

$$\Lambda_2 = \omega_l - 3r_l\delta\phi_k^{s2} - [3\epsilon\delta\phi_k^{s2} - p]k^2 < 0, \tag{18b}$$

with $\delta\phi_k^s = \sqrt{\frac{w_l+k^2p}{r_l+k^2\epsilon}}$. On the other hand, the one corresponding to the SHS's stability is

$$\Omega_k = -2\omega_l - k^2D^*(u^s) < 0. \tag{19}$$

Since now ω_l *can* be negative, the possible SHS are $u^s = 0$ when $\omega_l < 0$ and $u^s = \pm\sqrt{\frac{\omega_l}{r_l}}$ when $\omega_l > 0$. All these equations yield the same qualitative results as in the previous case. In this new context it is not only possible for a pattern to stabilize (even in absence of noise) but rather, there exists bistability under similar conditions as in the previous case (although for this circumstance the noise *is* necessary). This and other concepts become clearer by writing the stability equations for $\lambda = 0$. Those of the pattern's stability are

$$\Lambda_1 = -2\alpha < 0, \tag{20a}$$

$$\Lambda_2 = 2\alpha - 2pk^2 < 0, \tag{20b}$$

and those of the SHS's stability ($u^s = 0$ for this case) are

$$\Omega_k = -2\alpha + 2pk^2 < 0. \tag{21}$$

It turns out that the inequalities (20b) and (21) are mutually exclusive, thus bistability is ruled out. Bistability can only take place in the presence of a nonlinear term, be it of deterministic nature ($Q_b(u)$), of stochastic origin, [29] or both. Finally, a pattern can nonetheless stabilize even when none of these two processes is present, as a result of the aforementioned balance between the constructive process enabled by the attractive forces and the homogenization taken place by diffusion. It suffices to consider $\alpha = 0$ in the inequalities (20b) and (21), to visualize such a statement. In this case, the sign of p defines which of the two solutions (pattern or SHS) is stable. All these conclusions were checked by following the corresponding evolutions of $\phi_0(\tau)$ and $\delta\phi_k(\tau)$. Also we solved numerically the corresponding equation for the extended system. Although predicted, it was surprising to note that in the absence of any global force, a pattern can be sustained only by the balance between attractive forces and diffusion.

4. Conclusions

Along this work we have answered a series of questions raised in the introduction, and also during its development. It is by now clear that the pattern is built by the attractive forces and balanced by the diffusion process. The attractor may take part in this balance for small k, but for k large enough (still far below the inverse of the interaction range) it does not. Its true role is to destabilize the pattern, by pulling ϕ_0 toward it. This is in fact the mechanism through which a pattern can be destabilized, when the SHS is located in the DDP. Although we have discovered that moving the SHS toward the DAF is not strictly necessary to stabilize the pattern, it is true that this task is easier to achieve when the SHS is in such region, since the pattern is the only stable solution. But it is also true that when the SHS is located in the DDP, there can exist simultaneously more than one type of attraction basin (those of the SHS and those of the patterns). We saw that $p = \epsilon/4 - 1$ is the single most relevant parameter in defining the pattern's stability: $p > 0$ means that the DAF is enabled for some value of the field. When that happens, a band of k values can exist for which a pattern can be stabilized, when the interaction strength ϵ is strong enough.

In the general case, the noise has the double role of moving the SHS toward the DAF, where its destabilizing effect is eliminated, and to widen the band of stable modes toward larger k. But its role is more relevant in cases as the first one presented in this work (adsorption and desorption in metallic surfaces with lateral interactions), for which the nonlinearity is such that its presence becomes indispensable to stabilize the pattern. Contrarily, we saw that for the cubic nonlinearity this is not so: a pattern can be stabilized by the sole effect of the attractive forces. We even saw that a nonlinearity is not even necessary for this to happen. Moreover, in a system without any global force it was observed that a pattern can nonetheless be stabilized by the balance between attractive forces and diffusion.

Although the simplification of the extended model is only valid for approximately harmonic solutions, it rescues the essential processes intervening in the pattern formation mechanism. It allowed us to advance in the analytic calculation and it put into evidence facts that would otherwise remained hidden or at least, unclear. We were able to find transparent

expressions for the linear stability conditions of the pattern and to propose a more general application for this mechanism. A fact worth highlighting is that the relevant effects for the construction and stabilization of the pattern are captured by focusing on its extrema and zero. Such a proposal was confirmed by the later results, what enables to consider it in other contexts.

References

[1] M.C. Cross, P.C. Hohenberg, Rev. Mod. Phys. 65 (1993) 851.
[2] R. Kapral, K. Showalter (Eds.), Chemical Waves and Patterns, Kluwer, Dordrecht, 1993.
[3] J. Trost, T. Zambelli, J. Wintterlin, G. Ertl, Phys. Rev. B 54 (1996) 17850.
[4] J. Wintterlin, S. Völkening, T.V.W. Janssens, T. Zambelli, G. Ertl, Science 278 (1997) 1931.
[5] S. Völkening, K. Bedürftig, K. Jacobi, J. Wintterlin, G. Ertl, Phys. Rev. Lett. 83 (1999) 2672.
[6] S. Renisch, R. Schuster, J. Wintterlin, G. Ertl, Phys. Rev. Lett. 82 (1999) 3839.
[7] A. Mikhailov, G. Ertl, Chem. Phys. Lett. 238 (1994) 104.
[8] D. Battogtokh, M. Hildebrand, K. Krischer, A.S. Mikhailov, Phys. Rep. 288 (1997) 435.
[9] M. Hildebrand, A.S. Mikhailov, J. Phys. Chem. 100 (1996) 19089.
[10] M. Hildebrand, A.S. Mikhailov, G. Ertl, Phys. Rev. E 58 (1998) 5483.
[11] M. Hildebrand, A.S. Mikhailov, G. Ertl, Phys. Rev. Lett. 81 (1998) 2602.
[12] M. Hildebrand, Chaos 12 (2002) 144.
[13] L. Gammaitoni, P. Hänggi, P. Jung, F. Marchesoni, Rev. Mod. Phys. 70 (1998) 223.
[14] F. Sagués, J.M. Sancho, J. García-Ojalvo, Rev. Mod. Phys. 79 (2007) 829.
[15] P. Reimann, Phys. Rep. 361 (2002) 57.
[16] C. Van den Broeck, J.M.R. Parrondo, R. Toral, Phys. Rev. Lett. 73 (1994) 3395.
[17] C. Van den Broeck, J.M.R. Parrondo, R. Toral, R. Kawai, Phys. Rev. E 55 (1997) 4084.
[18] S.E. Mangioni, R.R. Deza, H.S. Wio, R. Toral, Phys. Rev. Lett. 79 (1997) 2389.
[19] S.E. Mangioni, R.R. Deza, R. Toral, H.S. Wio, Phys. Rev. E 61 (2000) 223.
[20] S.E. Mangioni, R.R. Deza, H.S. Wio, Phys. Rev. E 63 (2001) 041115.
[21] W. Horsthemke, R. Lefever, Noise Induced Transitions, Springer, Berlin, 1984.
[22] M. Ibañes, J. García-Ojalvo, R. Toral, J.M. Sancho, Phys. Rev. Lett. 87 (2001) 020601.
[23] O. Carrillo, M. Ibañes, J. García-Ojalvo, J. Casademunt, J.M. Sancho, Phys. Rev. E 67 (2003) 046110.
[24] J. Buceta, K. Lindenberg, Phys. Rev. E 69 (2004) 011102.
[25] J.M.R. Parrondo, C. Van den Broeck, J. Buceta, F.J. de la Rubia, Physica A 224 (1996) 153.
[26] J. Buceta, M. Ibañes, J.M. Sancho, K. Lindenberg, Phys. Rev. E 67 (2003) 021113.
[27] K. Wood, J. Buceta, K. Lindenberg, Phys. Rev. E 73 (2006) 022101.
[28] B. von Haeften, G.G. Izús, S.E. Mangioni, A.D. Sánchez, H.S. Wio, Phys. Rev. E 69 (2004) 021107.
[29] S.E. Mangioni, Physica A 389 (2010) 1799.
[30] S.B. Casal, H.S. Wio, S.E. Mangioni, Physica A 311 (2002) 443.
[31] M. Hildebrand, M. Kuperman, H.S. Wio, A.S. Mikhailov, G. Ertl, Phys. Rev. Lett. 83 (1999) 1475.
[32] S.E. Mangioni, H.S. Wio, Phys. Rev. E 71 (2005) 056203.
[33] S.E. Mangioni, R.R. Deza, Phys. Rev. E 82 (2010) 042101.